CLINICAL STUDY

Effectiveness of MRA on embolized intracranial aneurysms: a comparison of DSA, CE-MRA, and TOF-MRA

Ally Mohamed Qassim[1,2], Sheng Guan[2,*], Halfan Saidi Ngowo[3], Binghui Liu[2], Haowen Xu[2]

ABSTRACT

Purpose: The endovascular treatment of intracranial aneurysms was proven safe and effective compared to the alternative method of surgical clipping, despite the high recurrence rate. Follow-up of embolized intracranial aneurysms is mandatory for the early detection of recurrence and improved outcomes. DSA is used as the reference standard for this assessment. To determine the effectiveness of MRA in follow-up evaluations of intracranial aneurysms after embolization by comparing DSA, CE-MRA, and TOF-MRA.

Materials and Methods: Sixty-eight consecutive patients undergoing DSA, TOF-MRA, and CE-MRA during an interval of <1 week were enrolled in this 6-month study. Images were evaluated for occlusion status, patency of the parent vessels, and artifacts. The modified Raymond-Roy occlusion classification and Aneurysm Embolization Grades were used to assess the occlusion status and initial DSA images for detection of recurrence in two filtered study phases with optimized selection criteria. Seventeen observers (phase I: 9, phase II: 8) independently interpreted the double-blinded images. Agreement was expressed with a Fleiss kappa value; $p < 0.05$ was considered significant.

Results: This study included 68 patients with 77 aneurysms; 38 (49.35%) were treated with coil alone and 39 (50.65%) with stent-assisted coiling. In both phases, DSA was superior to TOF-MRA and CE-MRA using MRRC (Phase I: $k = 0.567$, $p \leq 0.001$; $k = 0.287$, $p \leq 0.001$; $k = 0.117$, $p \leq 0.001$, respectively; Phase II: $k = 0.503$, $p \leq 0.001$; $k = 0.303$, $p \leq 0.001$; $k = 0.115$, $p = 0.038$, respectively). TOF-MRA was as effective as DSA (TOF: $k = 0.335$, $p \leq 0.001$; DSA: $k = 0.323$, $p \leq 0.001$) for recurrence detection.

Conclusion: We suggest TOF-MRA as a first-line follow-up tool to detect aneurysm recurrence, and DSA to quantify the filling space to make a definite decision on re-embolization.

Key words: effectiveness; follow-up; intracranial aneurysms; MRA; DSA

[1]East Campus of Zhengzhou University, Zhengzhou, China.
[2]Department of Intervention Neuroradiology, The First Affiliated Hospital of Zhengzhou university, Zhengzhou, China.
[3]Department of Environmental Health and Ecological Science, Ifakara Health Institute, Ifakara, Morogoro, Tanzania.
Correspondence: Sheng Guan, MD, PhD, Director, Department of Intervention Neuroradiology, The First Affiliated Hospital of Zhengzhou University, Zhengzhou, 450052, China. Email: gsradio@126.com

Journal of Interventional Medicine 2018;1(1): 32-41.
DOI:10.19779/j.cnki.2096-3602.2018.01.08

INTRODUCTION

Since the publication of ISAT studies, endovascular management of unruptured and less complicated ruptured intracranial aneurysms (IAs) have become the treatment of choice over surgical management (1). This treatment has proven safe and effective despite having a high recurrence rate of 15–50% (2-5). Thus, follow-up of embolized IAs (EIAs) is mandatory to detect recurrence in early stages and improve outcomes. The ultimate goal of coil embolization is to promote thrombosis of the aneurysm sac and vascular remodeling across the neck (5). To achieve that goal and a good treatment outcome, several measures must be assessed and achieved. Among the most important measures are the degree of aneurysm occlusion after treatment, predictors of recurrence (recanalization), and predictors of bleeding and re-bleeding (4).

There are several classification systems in the literature that describe the appearance of the aneurysm and/or remnant filling after endovascular treatment of intracranial aneurysms. Roy *et al*. (6) and Raymond *et al.* (3) developed the Raymond-Roy occlusion classification (RROC): class 1 is complete obliteration, class 2 is residual neck, and class 3 is residual aneurysm.

As not all RROC-3 occlusions behave similarly, Mascitelli *et al.* (7) developed the modified Raymond–Roy classification (MRRC) to supplement the original RROC. The MRRC dichotomizes RROC class 3 occlusions into class 3a (residual aneurysm with contrast within the coil interstices) and class 3b (residual aneurysm with contrast along the aneurysm wall, neck, and wall of the sac). Stapleton *et al.* (4) conducted a validation of the MRRC using a retrospective cohort of EIAs and concluded that

MRRC is more useful than RROC for aneurysm assessment.

More clinical studies have shown an association of aneurysm recurrence with either homodynamic angiographic characteristics or aneurysm characteristics. In 2007, Deshaies *et al*. (8) proposed the Aneurysm Embolization Grade (AEG) as a tool for predicting aneurysm recurrence based on specific hemodynamic angiographic characteristics seen immediately after embolization. In 2013, Singla *et al.* (5) reported an internal validity study to evaluate the AEG described in Deshaies's study and speculated that non-invasive imaging cannot assess hemodynamic characteristics within the aneurysm as DSA can. This system includes classes AEG A (no filling of the aneurysm neck or dome), AEG B (contrast stasis in the neck, no filling of the dome), AEG C (contrast stasis in the neck and dome), AEG D (contrast flow in the neck, no filling of the dome), and AEG E (contrast flow in the neck and dome). Classes AEG D and E are more predictive of recurrence (5, 8). While the AEG system accounts for contrast stasis, it does not account for contrast location within the aneurysm dome as MRRC does (7).

DSA remains the gold standard for the identification and follow-up of clinically significant EIAs (9, 10). However, it is an invasive procedure with possible complications (11-14); a noninvasive angiographic method is desirable. Brain MRA performed while the patient is breathing freely and without the need for anesthesia has reached sufficient technical maturity to allow more widespread application of a standardized protocol. MRA meets all of the following criteria (15): Acceptable to the community, Feasible, Affordable [compared to DSA], Sustainable, and Safe to use with minimal contraindications and non-invasive (AFASS). Therefore, we conducted a study to determine the effectiveness of MRA for the follow-up evaluation of IAs after embolization by comparing DSA, CE-MRA, and TOF-MRA. We hypothesized that MRA could be used for follow-up evaluation of IAs after endovascular therapy to assess the embolization status and to help detect aneurysm recurrence. DSA was our reference test; CE-MRA and TOF-MRA were evaluated as index tests.

We assessed both CE-MRA and TOF-MRA for several reasons. First, some authors have reported that CE-MRA is better able to detect and accurately characterize embolized intracranial aneurysms (16). Second, others reported no significant differences between the modalities in the assessment of post-embolized intracranial aneurysms (17, 18). Finally, we wanted to evaluate both MRA techniques rather than a single technique to obtain more unequivocal results that might more clearly affect daily clinical practice.

MATERIALS AND METHODS

Study setting

A prospective cohort study including patients admitted to the Interventional Neuroradiology Department of the First Affiliated Hospital of Zhengzhou University was conducted. Patients were prospectively and consecutively selected and enrolled. DSA images of each patient acquired during the treatment of embolization of an intracranial aneurysm were retrospectively downloaded from the hospital PAC system and compared with current DSA, CE-MRA, and TOF-MRA images.

The inclusion criteria were: patients were admitted for follow-up of EIAs, patients were treated using the endovascular approach, and all angiographic methods were performed within an interval of < 1 week using the same machines. Exclusion criteria were: absence of initial/treatment DSA images (0), absence of MRA images (performed DSA only) (39), treatment with flow diverters (1), treatment with surgical clipping (2), and unavailability of image(s) in the PAC system (2). Our Institutional Review Board approved this study; written informed consent was obtained from all patients.

Between November 2015 and May 2016 (6 months), 112 patients were admitted for EIA follow-up. Only 68 patients meet all the inclusion criteria and were assessed in the initial phase (Phase I) of this study.

Image acquisition

Digital Subtraction Angiography Imaging

Intra-arterial DSA was performed using a biplane angiographic system (Philips, Allura, Xper, FD 20, Philips Healthcare, Amsterdam, the Netherlands). All DSA imaging was performed under general anesthesia. The following standard projections were obtained: anteroposterior, lateral, oblique, working views, and 3D images. Rotational angiograms were acquired within a single C-arm rotation of LAO 120 degrees to RAO 120 degrees [240 degrees] over 4.2 s. In other projections, the C-arm was at the maximum angle of approximately LAO 120 degrees and RAO 179 degrees. Selective injections of the internal carotid artery (ICA) or vertebral artery (VA) were performed according to the aneurysm location using transfemoral catheterization. For ICA, 7–8 mL of non-ionic contrast agent (iodixanol, Visipaque™, GE Healthcare, Oslo, Norway) was injected at a rate of 3–4 mL/s and a pressure of 300 psi. For the VA, 6–7 mL was injected at a rate of 2–3 mL/s and a pressure of 300 psi using an injector (MedRad, Mark V ProVis®, MEDRAD, USA).

Magnetic Resonance Angiography Imaging

MRA examinations were performed on a 3.0T Siemens magnet (Skyra, Siemens Medical Systems, Erlangen, Germany). Both TOF-MRA and CE-MRA were performed in the same imaging session using optimized parameters. TOF-MRA used the following: TE, 3.43 ms; TR, 21.0 ms; flip angle, 18 degrees; total acquisition time, 3:19 min; number of slabs, 3; slices per slab, 36; section thickness, 0.80 mm; FOV read, 220 mm; rectangular field of view (FOV phase), 90.6%; acquisition matrix, 0.87 × 0.57 × 1.60 mm; reconstructed voxel size, 0.3 × 0.3 × 0.8 mm. CE-MRA used the following: TE, 1.26 ms; TR, 3.39 ms; flip angle, 25 degrees; total acquisition time, 0:21 min; number of slabs, 1; slices per slab, 144; section

thickness, 0.80 mm; FOV read, 250 mm; rectangular field of view (FOV phase), 81.3%; acquisition matrix, 0.89 × 0.71 × 1.33 mm; reconstructed voxel size, 0.7 × 0.7 × 0.8 mm. CE-MRA randomly sampled the central k-space during venous injection of a gadolinium-based contrast agent at a dose of 0.1 mmol/kg (0.2 mL/kg) body weight. A bolus of 15–20 mL was used, followed by 20 mL saline at a rate of 1.5–2.0 mL/s and a maximum pressure of 325 psi for 23 s, with scopic-based detection of the bolus (phase contrast survey), using an MRI-compatible power-injector (Medrad® Spectris Solaris® EP MR Injection System, MEDRAD Medizinische Systeme GmbH, Volkach, Germany).

Image Reconstruction

All observers independently assessed the source images for both MRA modalities while knowing the number and location of the embolized aneurysms. The CE-MRA images included pre- and post-contrast sequences. The maximum intensity projections (MIPs) were present in all MRA image sequences, but observers were discouraged from using MIP for assessment due to signal loss. For DSA, the following standard projections were obtained: anteroposterior, lateral, oblique, working views, and 3D images.

Image Interpretation and Blinding Method

Each diagnostic modality was evaluated separately and independently by 17 experienced neuroradiologists (observers, 4-27 years of experience). Each observer interpreted the images of each patient in his or her group (MRA or DSA).

The study was staged in two phases (phase I and phase II) as a continuation of the outcome of interest: detection of aneurysm recurrence. Different methods of bias reduction were considered. *First,* each observer interpreted the images independently. *Second,* a comprehensive double-blinding method was used. *Third,* seminars on how to complete the forms (checklists) and image interpretations were conducted for each phase. *Fourth,* consent and an oath of confidentiality were obtained from all observers before image interpretation. *Fifth,* each observer received the images for the respective group on a pen drive. *Sixth,* all observers were requested to use their personal computers for image interpretation. *Seventh,* all observers received "RadiAnt DICOM viewer" software for image interpretation. *Eighth,* observers were allowed 4 weeks for interpretation in each phase. *Ninth,* optimized selection criteria were used to select phase II candidates from phase I. *Tenth,* only statistical inter-observer agreement (kappa statistics) was used to assess the consensus among members within a group (inter-observer agreement) and among groups (inter-modality agreement). *Last,* an independent statistician not affiliated with the hospital or the county analyzed the results.

A comprehensive double-blinding method was used. Observers from the MRA group were blinded to DSA images in both phases. Observers in the same group interpreted the images independently. The observers in phase I were different from those in phase II. Each group included members from different hospitals and departments. The observers within each group were mixed; the MRA group had members from different hospitals and departments, as did the DSA group. Neuroradiologists who performed the endovascular treatments were not involved in MRA image interpretation in phase II.

Phase I

Phase I of image interpretation included 9 observers: 5 in the MRA group and 4 in the DSA group.

The assessment tools used for each diagnostic modality were: MRRC, patency of parent vessels, no stenosis, mild stenosis (< 50%), moderate stenosis (50–69%), severe stenosis (70–99%), and occlusion (100%). The presence of artifacts in the images was classified as: no (absence of artifacts), minor (the artifacts did not inhibit image interpretation), or major (the artifacts inhibited image interpretation).

Selection Criteria for Phase II Image Interpretation

To our knowledge, no study has used a staging method. Therefore, there are no standard criteria for selection of candidates from one phase for inclusion in another. We used the following criteria for the selection of candidates for phase II: *One*, patients were classified as Class 2 or more [Class 2, 3a, or 3b] by 2 or more observers on TOF or CE-MRA; *Two*, patients were classified as Class 2 or more by 3 or more observers on both TOF and CE-MRA; *Three*, patients were classified as Class 2 or more by 2 or more observers on DSA. Two or more observers assessed the precision strength between the independent observers in clusters using statistical inter-observer agreement for consensus.

Phase II

Phase II image interpretation included 8 observers: 5 in the MRA group and 3 in the DSA group. Forty-seven patients with 48 EIAs were selected for phase II.

The MRA group members were given follow-up TOF-MRA and CE-MRA images and initial DSA images for interpretation. DSA group members were given initial and follow-up DSA images for interpretation. The MRRC and AEG systems were used for follow-up and initial DSA image interpretation, respectively.

The comparison of the two assessment tools was used to differentiate remnant from recurrence and to determine the aneurysm status in terms of detection of recurrence. Recurrence was defined as any increase in the size of the remnant and/or a change in the classification of the anatomic result (initial class) to a higher class (4). The aneurysms were classified as: absent (no recurrence), minor recurrence (very small, the size would theoretically not permit re-treatment with coils), and major recurrence (saccular, the size would theoretically permit re-treatment with coils) (3).

The criteria used to determine aneurysm status as recurrence based on MRRC classification of the follow-up images and AEG classification of the initial images were as follows: Class 1 and any grade (A, B, C, D, or E) was absent; class 2 and grade B or D was

absent (stable), or was recurrence if the size of the remnant increased; class 2 and grade C was recurrence, class 2 and grade E was absent, (stable) or was recurrence if the size of the remnant increased; class 3a and grade B or D was recurrence; class 3a and grade C or E was absent, (stable) or was recurrence if the size of the remnant increased; class 3b and grade B, C, D, or E was recurrence; class 3b and grade E was absent; class 2, 3a, or 3b and grade A was recurrence. Recurrence was classified as minor or major based on the theoretical size, as explained above.

Statistical Analysis

All statistical analyses were performed using the R Statistical Package (version 3.3.2 (2016-10-31)). All probability values were two-sided. A probability value of 0.05 (95% confidence interval) was considered significant. The levels of inter-observer and inter-modality agreement for evaluation of the angiographic images were analyzed using weighted kappa (k) statistics. As more than 3 observers were used for image interpretation, Fleiss kappa was used. The interpretation of kappa was: < 0, no agreement or poor agreement; 0–0.20, slight agreement; 0.21–0.40, fair agreement; 0.41–0.60, moderate agreement; 0.61–0.80, substantial agreement; 0.81–1.00, almost perfect agreement (19).

RESULTS

In the initial phase, 68 patients with 77 intracranial aneurysms were included in a 6-month prospective study of the follow-up of intracranial aneurysms after embolization. There were 42 (61.76%) females and 26 (38.24%) males aged 28–69 years, with a mean age of 53.58 ± 1.28 years. Forty-seven patients with 48 EIAs were selected for phase II. During follow-up, all patients underwent imaging with three angiographic diagnostic modalities within less than one week. Of the 77 aneurysms, 38 (49.35%) were treated by coil alone and 39 (50.65%) were treated by stent-assisted coiling.

Inter-observer and inter-modality agreement were analyzed using statistical methods to avoid biases that might affect the strength of the study.

Inter-observer and Inter-modality Agreement in Phase I

The agreements were calculated using Fleiss kappa statistics as described above. The kappa value and p-value show the strength of agreement. The paradoxical weighted kappa is the statistical discrepancy between the unadjusted level of agreement (quantified by the p-value) and the kappa value (20), in which there is high agreement and low kappa value (21). The paradox kappa is primarily due to poor precision and good accuracy among independent observers of the same group, and is usually associated with Fleiss kappa (21).

Fleiss kappa has low bound values compared to other multi-rater kappas (21, 22). We used the p-value to define significant agreement in all paradoxes.

The inter-observer and inter-modality agreements in phase I are shown in Tables 1 and 2, respectively. The findings revealed substantial to moderate agreement of the observers in the assessment of DSA images using MRRC to evaluate aneurysm occlusion status; the inter-modality (average) was moderate significant agreement ($k = 0.567$, $p \leq 0.001$). The CE-MRA had no to fair agreement when MRRC was used to evaluate aneurysm occlusion status; the average was slight significant agreement ($k = 0.117$, $p \leq 0.001$). There was fair to moderate agreement among observers for the usefulness of TOF-MRA for the evaluation of aneurysm embolization status using MRRC; the average was fair significant agreement ($k = 0.287$, $p \leq 0.001$). Analysis of the calculated kappa values indicated that DSA was superior to both TOF-MRA and CE-MRA, and TOF-MRA was superior to CE-MRA (DSA > TOF-MRA > CE-MRA). All modalities were significant ($p < 0.001$) in clinical practice.

The results of the parent vessel patency assessment tool revealed no to substantial observer agreement in the interpretation of DSA images for evaluation of parent vessel patency, with an average of fair significant agreement ($k = 0.287$, $p \leq 0.001$). CE-MRA had no to slight agreement, with an average of slight significant agreement ($k = 0.079$, $p \leq 0.001$). However, it had a no to fair range of agreement among observers evaluating its usefulness on TOF-MRA, with an average of slight significant agreement ($k = 0.164$, $p \leq 0.001$). No observer interpreted moderate stenosis on DSA images. Nevertheless, the consensus of the observers for CE- and TOF-MRA was almost similar, with slight nonsignificant agreement ($k = 0.009$, $p = 0.801$; $k = 0.02$, $p = 0.584$, respectively). There was substantial significant agreement among all observers when using DSA images to interpret occlusion ($k = 0.797$, $p \leq 0.001$), and strong disagreement when using MRA to determine vessel occlusion. Analysis of the calculated kappa values revealed that DSA was superior to both TOF-MRA and CE-MRA, while TOF-MRA was superior to CE-MRA (DSA > TOF-MRA > CE-MRA). All modalities were significant ($p < 0.001$) in clinical practice.

DSA demonstrated highly significant usefulness among observers for the identification of images with no artifact ($k = 0.202$, $p \leq 0.001$) and major artifact ($k = 0.329$, $p \leq 0.001$), while CE-MRA was useful for the expression of minor artifacts ($k = 0.953$, $p \leq 0.05$). TOF-MRA images were less likely to have artifacts ($k = 0.9$, $p \leq 0.05$).

Table 1 Inter-observer agreement of phase I patients

	DSA			CE-MRA			TOF-MRA		
	kappa	z-value	p-value[a]	kappa	z-value	p-value[a]	kappa	z-value	p-value[a]
MRRC									
Class 1	0.666	14.32	<0.001	0.178	4.836	<0.001	0.314	0.552	<0.001
Class 2	0.504	10.829	<0.001	-0.025	-0.683	0.495	0.229	6.234	<0.001
Class 3a	0.489	10.503	<0.001	0.022	0.592	0.554	0.095	2.59	<0.05
Class 3b	0.429	9.214	<0.001	0.228	6.213	<0.001	0.53	14.417	<0.001
Vessel patency									
No stenosis	0.276	5.929	<0.001	0.147	4.003	<0.001	0.205	5.568	<0.001
Mild stenosis	-0.023	-0.5	0.617	-0.027	-0.73	0.466	0.115	3.118	<0.05
Moderate stenosis				0.009	0.252	0.801	0.02	0.548	0.584
Severe stenosis	0.215	4.612	<0.001	0.168	4.579	<0.001	0.222	6.047	<0.001
Occlusion	0.797	17.124	<0.001	-0.028	-0.756	0.450	-0.019	-0.525	0.6
Artifacts									
No	0.202	4.338	<0.001	0.036	0.992	0.321	0.09	2.445	<0.05
Minor	0.075	1.614	0.107	0.093	2.543	<0.05	0.064	1.749	0.08
Major	0.329	7.071	<0.001	0.061	1.659	0.097	-0.005	-0.148	0.882

Abbreviations: DSA, digital subtraction angiography; CE-MRA, contrast-enhanced magnetic resonance angiography; TOF-MRA, time-of-flight magnetic resonance angiography; MRRC, modified Raymond-Roy occlusion classification.
[a] Statistically significant p-value used was <0.05.

Table 2 Inter-modality agreements for phase I included patents.

Variables	Kappa	Z-value	P-value[a]
MRRC			
DSA	0.567	16.8	<0.001
CE-MRA	0.117	4.91	<0.001
TOF-MRA	0.287	12.2	<0.001
Vessels patency			
DSA	0.287	8.6	<0.001
CE-MRA	0.0789	3.33	<0.001
TOF-MRA	0.164	6.81	<0.001
Artifacts			
DSA	0.157	3.75	<0.001
CE-MRA	0.063	2.17	<0.05
TOF-MRA	0.0742	2.14	<0.05

DSA, indicates for Digital Subtraction Angiography; CE-MRA, Contrast-enhanced Magnetic resonance angiography; TOF-MRA, Time of flight Magnetic resonance angiography; MRRC, Modified Raymond-Roy occlusion classification.
[a] Statistically significant p-value used was <0.05.

Inter-observer and Inter-modality Agreement in Phase II

Independent observers blinded to phase I results were used to confirm the MRRC classification of selected patients. There was slight to substantial agreement in the DSA group; the use of DSA in the diagnosis of class 1, 2, and 3b aneurysm occlusion status was highly significant. The TOF-MRA group had slight to moderate agreement, with significance similar to DSA, while the CE-MRA group had nonsignificant agreement. Thus, TOF-MRA ($k = 0.303$, $p \leq 0.001$) was superior to CE-MRA ($k = 0.115$, $p = 0.038$), while DSA ($k = 0.503$, $p \leq 0.001$) continued to be the reference method for EIA assessment even when using MRRC classification. Tables 3 and 4 include details of phase II inter-observer and inter-modality agreement, respectively.

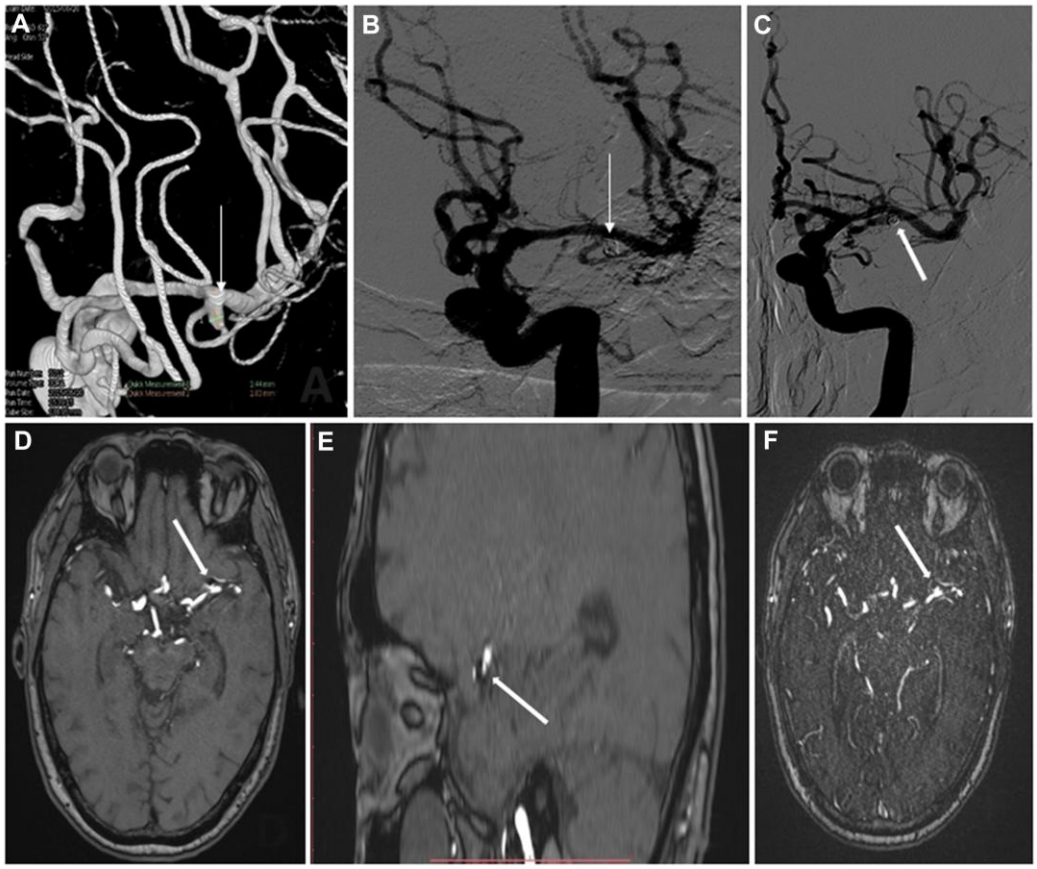

Figure 1. Case of a stable remnant (no recurrence). (A) Patient with a left middle cerebral artery (MCA) aneurysm (AEG grade C) treated with coil alone. (B) A DSA image obtained immediately after treatment shows a neck remnant (arrow) intentionally left to supply the branch artery. (C) DSA, (D-E) TOF-MRA and, (F) CE-MRA images obtained 9 months after treatment indicated the neck remnant was stable (no increase in size, thick arrows). Many observers interpreted the aneurysm as a class 2 on each imaging modality, but there was very strong agreement among observers for the interpretation of the TOF-MRA images.

Among the three observational groups, the TOF-MRA group had a higher agreement for assessment of the initial DSA images using AEG than the DSA and CE-MRA groups. However, the DSA group detected grades A and E more precisely (k = 0.713, k = 0.427, respectively).

Detection of recurrence revealed: the TOF-MRA observers were better able to detect absent, minor, and major recurrence of aneurysms (Figure 1). However, DSA observers were able to more precisely exclude recurrence (k = 0.407) compared to either MRA modality (TOF-MRA: k = 0.289; CE-MRA: k = 0.036). All observers were able to detect major recurrences with moderate precision (DSA: k = 0.468; TOF-MRA: k = 0.486; CE-MRA: k = 0.534) (Figure 2). TOF-MRA was as effective as DSA (TOF: k = 0.335: $p \leq 0.001$; DSA: k = 0.323, $p \leq 0.001$) for the detection of recurrence of EIAs, although all modalities were clinically very useful.

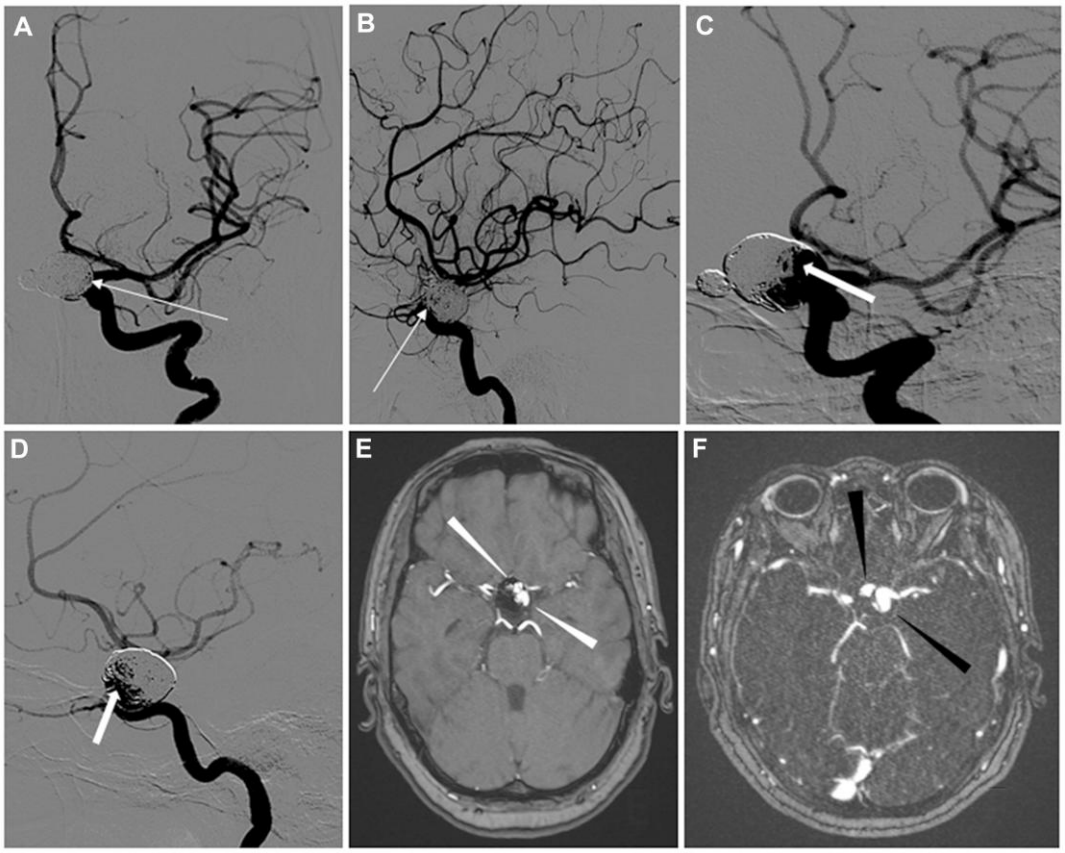

Figure 2. Exemplary case of major recurrence due to coil compaction. A patient with a left internal carotid artery (ICA) aneurysm (AEG grade C) embolized with a coil alone. (A-B) DSA images obtained immediately after treatment show complete aneurysm occlusion with a thrombus at the neck of the aneurysm (arrows), the contrast material visualized during the capillary and (B) early venous phases. (C-D) DSA images obtained 22 months after treatment showed an increase in the neck remnant and a newly formed dome wall remnant (class 3b); the coils are highly compacted (thick arrows). (E) TOF-MRA and (F) CE-MRA images obtained at the same time as the DSA images show class 3b flow residue (arrow heads). Note: a small coiled aneurysm beside the large aneurysm is located on the right ICA and shows complete stable occlusion.

Table 3 Inter-observer agreement for the detection of recurrent aneurysms in phase II

	DSA group			CE-MRA group			TOF-MRA group		
	kappa	**z-value**	**p-value[a]**	**kappa**	**z-value**	**p-value[a]**	**kappa**	**z-value**	**p-value[a]**
MRRC confirmation[b]									
Class 1	0.682	7.661	<0.001	0.085	0.947	0.344	0.395	6.270	<0.001
Class 2	0.572	6.423	<0.001	0.054	0.597	0.550	0.371	5.893	<0.001
Class 3a	0.142	1.597	0.110	0.143	1.583	0.114	0.107	1.702	0.089
Class 3b	0.228	2.560	0.010	0.148	1.640	0.101	0.274	4.357	<0.001
AEG grade[c]									
Grade A	0.713	8.005	<0.001	0.073	0.814	0.416	0.274	4.357	<0.001
Grade B	0.132	1.485	0.137	-0.034	-0.373	0.709	0.130	2.059	0.039
Grade C	0.131	1.471	0.141	-0.016	-0.178	0.858	0.287	4.557	<0.001
Grade D	-0.125	-1.403	0.161	0.170	1.882	0.060	0.268	4.250	<0.001
Grade E	0.427	4.796	<0.001	0.214	2.375	0.018	0.236	3.744	<0.001
Recurrence detection									
Absent	0.407	4.569	<0.001	0.036	0.397	0.691	0.289	4.588	<0.001
Minor	0.082	0.916	0.359	-0.033	-0.363	0.716	0.287	4.557	<0.001
Major	0.468	5.255	<0.001	0.534	5.923	<0.001	0.486	7.711	<0.001

Abbreviations: DSA, digital subtraction angiography; CE-MRA, contrast-enhanced magnetic resonance angiography; TOF-MRA, time-of-flight magnetic resonance angiography; MRRC, modified Raymond-Roy occlusion classification
[a] Statistically significant p-value used was <0.05.
[b] second assessment of selected patients from phase I to confirm the occlusion status of aneurysms in blinding methods.

Table 4 Inter-modality agreements for detection of recurrent aneurysm, observed in phase II of the study.

Variables	kappa	z-value	p-value[a]
MRRC confirmation[b]			
DSA	0.503	8.56	<0.001
CE-MRA	0.115	2.08	0.0377
TOF-MRA	0.303	8.2	<0.001
AEG grades			
DSA	0.362	7.16	<0.001
CE-MRA	0.115	2.26	0.024
TOF-MRA	0.246	7.44	<0.001
Recurrence detection			
DSA	0.323	4.93	<0.001
CE-MRA	0.132	2.01	0.0446
TOF-MRA	0.335	7.23	<0.001

DSA, indicates for Digital Subtraction Angiography; CE-MRA, Contrast-enhanced Magnetic resonance angiography; TOF-MRA, Time of flight Magnetic resonance angiography; MRRC, Modified Raymond-Roy occlusion classification.
[a]Statistically significant p-value used was <0.05.
[b]second assessment of selected patients from phase I to confirm the occlusion status of aneurysms in blinding methods.

DISCUSSION

Although several studies on the effectiveness of MRA in comparison to DSA for the follow-up evaluation of EIAs have been published, the data in this study are the first to include randomly selected patients, 17 observers to interpret angiographic images in a comprehensive double-blinded manner, and filtered phases. Also, this may be the first study to describe the aneurysm embolization status on MRA images using MRRC, and to clearly detect aneurysm recurrence using MRRC classification on follow-up angiographic images in comparison to AEG classification of the initial DSA images.

To our knowledge, this is the only study that used Fleiss kappa statistics to assess the variability among the observers and modalities due to the involvement of more than three observers in each stage of the study. Kappa is affected by the prevalence and the number of observers (20). Most studies used Cohen's kappa statistic (23) for less than three observers, and the multi-rater derivative Hubert kappa for more than three observers (22).

DSA has been the traditional reference standard imaging modality for the assessment of aneurysm status during follow-up after endovascular management (17, 24, 25). However, DSA has been replaced by non-invasive angiographic modalities for EIA assessment and the detection of recurrence without a standard guideline during long-term follow-ups (17, 24, 25).

The present study used DSA as a reference standard to evaluate the diagnostic impact of two different MRA techniques on treatment decisions, and focused on changes in clinical practice.

Our study revealed that TOF-MRA is superior to CE-MRA for the evaluation of EIAs using MRRC. Similar findings were reported by a study using another aneurysm occlusion classification method (26) to evaluate EIAs on MRA. In contrast, several authors have reported the superiority of CE-MRA over TOF-MRA for EIA evaluation (18, 27, 28). Moreover, TOF-MRA has a high spatial resolution and signal-to-noise ratio, which increases the clarity of images compared to CE-MRA (29, 30). DSA has higher agreement on vessel evaluation than TOF-MRA or CE-MRA, which may be due to the high quality of vessel visualization (31).

Medical imaging artifacts are the most common cause of misinterpretation of images and misdiagnosis (32, 33). According to our study, the DSA images of some patients had major artifacts, which might lead to misinterpretation of images and decrease the diagnostic accuracy. The metal artifacts in DSA can be reduced using high-resolution C-arm CT (34, 35) and an increased volume of contrast media (36). In our study, most images demonstrated artifact-free DSA and TOF-MRA images. Minor artifacts were visible in CE-MRA images. This was different from other reports, in which CE-MRA images were free of artifacts compared to TOF-MRA images (29). The most important mechanisms for artifact formation are the interference of metal-induced field disturbances, intra-voxel dephasing leading to signal loss in areas of strong local magnetic fields around the metallic implant (33), and motion artifacts (37).

In our results, TOF-MRA images were more significant than DSA or CE-MRA for detection of absent, minor and major recurrence of aneurysms. In a meta-analysis, Amerongen *et al*. (17) reported similar results. This may be explained by the observers' overestimation due to a T1-hyperintense thrombus within aneurysms on TOF-MRA images (38), and the presence of the helmet phenomenon, which usually affects DSA images (39). It is also contrary to other studies that reported CE-MRA to be superior to DSA alone (40) and to both DSA and TOF-MRA (27, 41).

Furthermore, the current study described the ability of DSA to precisely exclude recurrence compared to

both MRA techniques. However, all angiographic modalities were moderately precise in the detection of major recurrences.

In addition, a well-trained and experienced observer was also an important factor in the diagnostic accuracy of image interpretation. Higher agreement was observed among images interpreted by experienced observers compared to less experienced observers (42, 43). The observers in our study had a wide range of experience, which might be a reason for the high discrepancies among observers in the same group, and may have caused low precision and decreased agreement. This can also explain the disagreement among observers in the interpretation of a new AEG grade in initial DSA image assessment and MRRC in MRA images.

This study has several limitations. It was a single-centered, short-term, prospective study. The observers had a wide range of experience, and there were Fleiss kappa paradoxes due to the many independent observers and categories.

TOF-MRA is a non-invasive technique that shows promising diagnostic effectiveness for the detection of EIA recurrence during follow-up. Despite this, all modalities are very useful in clinical practice, but DSA will remain the reference modality. CE-MRA is less effective than TOF-MRA. We consider TOF-MRA to be a first-line modality screening tool for follow-up to detect aneurysm recurrence. However, once recurrence has been detected, we suggest that it be confirmed using DSA to quantify the filling space and make a definite decision on re-embolization. A TOF-MRA finding of no residual generally does not require DSA confirmation.

Several improvements can be included in future studies. A multi-center, longitudinal, long-term prospective study with effective blindness techniques will have increased strength. Neuroradiologists should be encouraged to evaluate EIAs using MRRC classification in daily clinical practice, and a method to resolve paradox agreements should be found.

References

1. Bunc G, Ravnik J, Vorsic M, et al. Endovascular versus operative treatment of cerebral aneurysms: a comparison of results from a low-volume neurosurgical centre. Wien Klin Wochenschr 2016; 128: 354-359.
2. Leng B, Zheng Y, Ren J, et al. Endovascular treatment of intracranial aneurysms with detachable coils: correlation between aneurysm volume, packing, and angiographic recurrence. J Neurointerv Surg 2014; 6: 595-599.
3. Raymond J, Guilbert F, Weill A, et al. Long-term angiographic recurrences after selective endovascular treatment of aneurysms with detachable coils. Stroke 2003; 34: 1398-1403.
4. Stapleton CJ, Torok CM, Rabinov JD, et al. Validation of the Modified Raymond-Roy classification for intracranial aneurysms treated with coil embolization. J Neurointerv Surg 2016; 8: 927-933.
5. Singla A, Villwock MR, Jacobsen W, et al. Aneurysm embolization grade: a predictive tool for aneurysm recurrence after coil embolization. Acta Neurochir (Wien) 2013; 155: 231-236.
6. Roy D, Milot G, Raymond J. Endovascular treatment of unruptured aneurysms. Stroke 2001; 32: 1998-2004.
7. Mascitelli JR, Moyle H, Oermann EK, et al. An update to the Raymond-Roy Occlusion Classification of intracranial aneurysms treated with coil embolization. J Neurointerv Surg 2015; 7: 496-502.
8. Deshaies EM, Adamo MA, Boulos AS. A prospective single-center analysis of the safety and efficacy of the hydrocoil embolization system for the treatment of intracranial aneurysms. J Neurosurg 2007; 106: 226-233.
9. Kaufmann TJ, Huston J, 3rd, Mandrekar JN, et al. Complications of diagnostic cerebral angiography: evaluation of 19,826 consecutive patients. Radiology 2007; 243: 812-819.
10. Dawkins AA, Evans AL, Wattam J, et al. Complications of cerebral angiography: a prospective analysis of 2,924 consecutive procedures. Neuroradiology 2007; 49: 753-759.
11. Orru E, Roccatagliata L, Cester G, et al. Complications of endovascular treatment of cerebral aneurysms. Eur J Radiol 2013; 82: 1653-1658.
12. AbuRahma AF, Hayes JD, Deel JT, et al. Complications of diagnostic carotid/cerebral arteriography when performed by a vascular surgeon. Vasc Endovascular Surg 2006; 40: 189-195.
13. Burger IM, Murphy KJ, Jordan LC, et al. Safety of cerebral digital subtraction angiography in children: complication rate analysis in 241 consecutive diagnostic angiograms. Stroke 2006; 37: 2535-2539.
14. Thiex R, Norbash AM, Frerichs KU. The safety of dedicated-team catheter-based diagnostic cerebral angiography in the era of advanced noninvasive imaging. AJNR Am J Neuroradiol 2010; 31: 230-234.
15. Adegbehingbe SM, Paul-Ebhohimhen V, Marais D. Development of an AFASS assessment and screening tool towards the prevention of mother-to-child HIV transmission (PMTCT) in sub-Saharan Africa--a Delphi survey. BMC Public Health 2012; 12: 402.
16. Kaufmann TJ, Huston J, 3rd, Cloft HJ, et al. A prospective trial of 3T and 1.5T time-of-flight and contrast-enhanced MR angiography in the follow-up of coiled intracranial aneurysms. AJNR Am J Neuroradiol 2010; 31: 912-918.
17. van Amerongen MJ, Boogaarts HD, de Vries J, et al. MRA versus DSA for follow-up of coiled intracranial aneurysms: a meta-analysis. AJNR Am J Neuroradiol 2014; 35: 1655-1661.
18. Lubicz B, Levivier M, Sadeghi N, et al. Immediate intracranial aneurysm occlusion after embolization with detachable coils: a comparison between MR angiography and intra-arterial digital subtraction angiography. J Neuroradiol 2007; 34: 190-197.
19. Landis JR, Koch GG. The measurement of observer agreement for categorical data. Biometrics 1977; 33: 159-174.
20. Viera AJ, Garrett JM. Understanding interobserver agreement: the kappa statistic. Fam Med 2005; 37: 360-363.
21. Falotico R, Quatto P. Fleiss' kappa statistic without paradoxes. Qual Quant 2015; 49: 463-470.
22. Warrens MJ. Inequalities between multi-rater kappas. Adv Data Anal Classif 2010; 4: 271-286.
23. Kundel HL. Polansky M. Measurement of Observer Agreement Radiology 2003; 228: 303-308.
24. Weng HH, Jao SY, Yang CY, et al. Meta-analysis on Diagnostic Accuracy of MR Angiography in the Follow-Up of Residual Intracranial Aneurysms Treated with Guglielmi Detachable Coils. Interv Neuroradiol 2008; 14 Suppl 2: 53-63.
25. Bakker NA, Westerlaan HE, Metzemaekers JD, et al. Feasibility of magnetic resonance angiography (MRA) follow-up as the primary imaging modality after coiling of intracranial aneurysms. Acta Radiol 2010; 51: 226-232.
26. Wu Q, Li MH. A comparison of 4D time-resolved MRA with keyhole and 3D time-of-flight MRA at 3.0 T for the evaluation of cerebral aneurysms. BMC Neurol 2012; 12: 50.
27. Serafin Z, Strzesniewski P, Lasek W, et al. Comparison of remnant size in embolized intracranial aneurysms measured at follow-up with DSA and MRA. Neuroradiology 2012; 54: 1381-1388.
28. Levent A, Yuce I, Eren S, et al. Contrast-Enhanced and Time-of-Flight MR Angiographic Assessment of Endovascular Coiled Intracranial Aneurysms at 1.5 T. Interv Neuroradiol 2014; 20: 686-692.
29. Lu H, Nagae-Poetscher LM, Golay X, et al. Routine clinical brain MRI sequences for use at 3.0 Tesla. J Magn Reson Imaging 2005; 22: 13-22.
30. Anzalone N. Contrast-enhanced MRA of intracranial vessels. Eur Radiol 2005; 15 Suppl 5: E3-10.

31. Cho YD, Kim KM, Lee WJ, et al. Time-of-flight magnetic resonance angiography for follow-up of coil embolization with enterprise stent for intracranial aneurysm: usefulness of source images. Korean J Radiol 2014; 15: 161-168.
32. Agid R, Schaaf M, Farb R. CE-MRA for follow-up of aneurysms post stent-assisted coiling. Interv Neuroradiol 2012; 18: 275-283.
33. Schaafsma JD, Velthuis BK, Vincken KL, et al. Artefacts induced by coiled intracranial aneurysms on 3.0-Tesla versus 1.5-Tesla MR angiography--An in vivo and in vitro study. Eur J Radiol 2014; 83: 811-816.
34. Yuki I, Kambayashi Y, Ikemura A, et al. High-Resolution C-Arm CT and Metal Artifact Reduction Software: A Novel Imaging Modality for Analyzing Aneurysms Treated with Stent-Assisted Coil Embolization. AJNR Am J Neuroradiol 2016; 37: 317-323.
35. Prell D, Kyriakou Y, Struffert T, et al. Metal artifact reduction for clipping and coiling in interventional C-arm CT. AJNR Am J Neuroradiol 2010; 31: 634-639.
36. Pjontek R, Onenkoprulu B, Scholz B, et al. Metal artifact reduction for flat panel detector intravenous CT angiography in patients with intracranial metallic implants after endovascular and surgical treatment. J Neurointerv Surg 2016; 8: 824-829.
37. Li MH, Li YD, Gu BX, et al. Accurate diagnosis of small cerebral aneurysms </=5 mm in diameter with 3.0-T MR angiography. Radiology 2014; 271: 553-560.
38. Gramsch C, Zulow S, Nensa F, et al. Can we now dispense with DSA in the evaluation of aneurysm occlusion even in the most crucial first follow-up after endovascular treatment? Clin Neurol Neurosurg 2016; 149: 136-142.
39. Agid R, Willinsky RA, Lee SK, et al. Characterization of aneurysm remnants after endovascular treatment: contrast-enhanced MR angiography versus catheter digital subtraction angiography. AJNR Am J Neuroradiol 2008; 29: 1570-1574.
40. Shankar JJ, Lum C, Parikh N, et al. Long-term prospective follow-up of intracranial aneurysms treated with endovascular coiling using contrast-enhanced MR angiography. AJNR Am J Neuroradiol 2010; 31: 1211-1215.
41. Marciano D, Soize S, Metaxas G, et al. Follow-up of intracranial aneurysms treated with stent-assisted coiling: Comparison of contrast-enhanced MRA, time-of-flight MRA, and digital subtraction angiography. J Neuroradiol 2017; 44: 44-51.
42. White PM, Wardlaw JM, Lindsay KW, et al. The non-invasive detection of intracranial aneurysms: are neuroradiologists any better than other observers? Eur Radiol 2003; 13: 389-396.
43. Carletta J. Assessing agreement on classification tasks: the kappa statistic. Comput Linguist 1996; 22: 249-254.